On CSI and Passive WiFi Radar for Opportunistic Physical Activity Recognition

Wenda Li*, Mohammud J. Bocus †, Chong Tang*, Robert. J. Piechocki†, Karl Woodbridge‡, Kevin Chetty*

*Department of Security and Crime Science, University College London, UK
†Department of Electrical and Electronic Engineering, University of Bristol, UK
‡Department of Electronic and Electrical Engineering, University College London, UK
{wenda.li, chong.tang.18, k.woodbridge, k.chetty}@ucl.ac.uk, {junaid.bocus,r.j.piechocki}@bristol.ac.uk

***Abstract*—The use of WiFi signals for human sensing has gained significant interest over the past decade. Such techniques provide affordable and reliable solutions for healthcare-focused event detection such as prevention of falls and long-term monitoring of chronic diseases. Currently, there are two major approaches for WiFi sensing: Passive WiFi Radar (PWR) which uses well established approaches from bistatic radar, and Channel State Information (CSI) which comes from the WiFi communication system. However, to our knowledge there has not been a comprehensive study to understand and compare both approaches in terms of their robustness and limitations for monitoring the movements of people. In this paper, we describe the fundamentals of both the CSI and PWR systems and the associated signal processing methodologies. To facilitate a direct-comparison between CSI and PWR, we have implemented a monitoring system for simultaneously measuring human activity using both techniques in comparable conditions. Experimental results show that CSI system works better in line-of-sight condition, whereas PWR system works better in non-line-of-sight condition. CSI system is more sensitive to the small activities, while PWR system provides meaningful Doppler spectrograms. It is therefore recommended that a real-world future WiFi system should leverage the fusion of the two approaches.**

***Index Terms*—Passive WiFi Radar, Channel State Information, Doppler, Wireless Sensing**

I. Introduction

With a fast growing global ageing population, there are increasing concerns that health conditions such as cardiovascular diseases, mental health issues and diabetes will become more prevalent and increase the burden on national healthcare services. Hence there is a greater need than ever to provide efficient technologies solutions for ambient assisted living and e-healthcare services [1]. Daily activity and behavior sensing in residential areas and care homes can provide invaluable information for both long-term and short-term tasks such as monitoring the daily routine of a user and identifying any discrepancy in their everyday behavior which may be due to illness or any other serious health conditions. Such systems are extremely helpful for improving quality of life and preventing health risks where early interventions are critical. Compared to other technologies used in healthcare monitoring such as cameras and wearable sensors, WiFi based sensing technology is considered as an ideal solution because it does not produce images or identify people being monitored thus alleviates privacy concerns. Furthermore, it performs uncooperative sensing so does not requires the use of wearable technology which has a low compliance rate, especially amongst the elderly, and may be uncomfortable and unsuitable for some users (e.g. those with skin conditions). Nowadays, WiFi devices are readily available in almost all indoor environments, whether residential or commercial, and they have become a potential candidate for wireless sensing mainly due to their non-intrusive nature and they require no additional infrastructure. For indoor sensing applications, WiFi based approaches have been used for activity and gait recognition [2], fall detection [3], gesture recognition [4], and intrusion detection [5].

The main concept behind WiFi sensing is that a moving person will affect the communication channel of a WiFi signal in terms of frequency shift, propagation paths and signal attenuation. As a result, the characteristics of communication channel becomes time-varying with the human activity and hence can be exploited for monitoring purposes.

Device-free sensing may be categorized into radar-based (Doppler), Received Signal Strength (RSS) and Channel State Information (CSI). The latter provides both amplitude and phase information. The phase can be used to obtain the Angle of Arrival (AoA), Time of Flight (ToF) and Time Difference of Arrival (TDoA). The purposes of these information are varied. For example, RSS has been widely used for indoor localization using the Finger-Printing (FP) method [6], where the RSS Indicator (RSSI) is compared to an offline pre-computed radio map (database). However, any changes in the environment will require a re-calibration to the database which is a time-consuming and complex process, and limits real-world applications. AoA is another useful information which is obtained by calculating the phase difference of the signals arriving at multiple antennas [7]. However, the AoA technique cannot be directly used in WiFi passive sensing applications, as it is based on the direction of arrival of the signal from the transmitter to the receiver (WiFi AP). Therefore, the user should usually be equipped with a transmitting WiFi device for the receiver to detect his/her position. ToF gives the relative distance between the transmitter and receiver by calculating the arrival time of the direct wave [8]. In a WiFi system, using ToF information only for localisation is quite challenging since it is influenced by the bandwidth. For instance, with the low sampling rates of the 20 and 40 MHz channel bandwidths

(50 ns and 25 ns time resolution, respectively), the direct signal may arrive between sampled intervals, giving rise to distance estimation errors in the order of several meters. Our previous work [9] shows the potential of PWR to detect small movements of the chest wall in signs-of-life detection. Moreover, our prototype system has been further extended for micro-Doppler based activity event classification [10]. WiFi CSI, which can be retrieved from a few IEEE 802.11n NIC, represents how wireless signals propagate from the transmitter to the receiver at a given carrier frequency across multiple paths [5]. CSI has been used in many applications like activity recognition [11], finger gesture recognition [12] and people counting [13].

In this paper, we focus on the two major approaches for activity recognition, the PWR system which outputs target Doppler information and the CSI system which provides data relating to the characteristics of the channel. Two systems have been implemented to demonstrate the feasibility of each approach. Experimental data has been collected simultaneously and timestamped using Network Time Protocol (NTP) Servers for synchronization. We demonstrate the detection results from both systems using six different activities performed by five people. After, we briefly discuss the difference between the two systems in terms of geometrical considerations, application potential and resilience to environmental changes. Although both the CSI and PWR systems can provide meaningful results for human activity recognition, there are still many challenges that need to be solved before real-world deployment. Compared to previous WiFi CSI [4], [5], [19] and passive WiFi radar [9], [17], [18] studies, this work makes the following contributions:

- To the best of the authors' knowledge, this is the first work to demonstrate the difference between CSI and PWR systems where experimental data is collected from a real-world scenario.
- We have setup two systems for WiFi CSI and passive WiFi radar to facilitate a direct comparison. Experimental results evaluate the difference between the two systems, and identify the layout and coverage sensitivities.
- We have discussed CSI and PWR in terms of their advantages and limitations in system development and deployment. We have also assessed potential future improvements for WiFi sensing.

This paper is organized as follow: Related works are presented in Section II; An overview of the WiFi signal is given in Section III; The signal processing for the CSI system is described in Section IV; The signal processing for the PWR system is explained in Section V; The system design and evaluation are presented in Section VI; Section VII discusses the feasibility and limitations of the two approaches; Finally, conclusions are drawn in Section VIII.

II. Related Work

In this section, we compare the previous works for both the PWR and CSI systems. Generally, Doppler information can be obtained from the PWR data. However, the way the two systems extract this information is vastly different. A comparison of these works is shown in Table I.

A. WiFi CSI System

For a WiFI system with MIMO-OFDM capability, its CSI is obtained as a 3D matrix, consisting of complex values which can be broken down into amplitude and phase information [5]. CSI measurements in the time domain capture the changes in the wireless signal due to the latter's interaction with surrounding objects or human activities and the observed patterns can be used for various purposes. Different WiFi sensing applications have specific requirements in terms of their signal processing techniques and classification/estimation algorithms.

For example, [6] presents a compressive sensing based FP for indoor localization by using the RSS information. However, the radio map is very time consuming to build and needs calibration when the environment changes, which limits its potential application in a residential environment. The authors in [12] employ CSI for fine-grained finger gesture recognition by using the principal component as the feature and dynamic time warping (DTW) as the classifier. They claim to achieve an accuracy of 95% on 8 finger gestures compared to 76% using RSS information. The idea of [12] is that subcarriers in OFDM signal are highly sensitive to the small movements in the physical environment which result in changes in the CSI. The latter has also been used in device-free activity recognition [2], [14]. For example, [14] proposes a CSI-speed model to quantify the relationship between CSI dynamics and human movement speed. The frequency component is extracted from the CSI using Discrete Wavelet Transform (DWT) and Hidden Markov Model (HMM) is used to build the CSI-activity model to classify human activities. Another work [2] uses the Short-Time Fourier Transform (STFT) technique to transform the CSI measurements into spectrograms. The torso speed and cycle time of each gait are calculated and used as features in a SVM classifier, achieving an accuracy of 92% for a human walking at a distance of 14 m. Fall detection is another important area in WiFi sensing. For instance, [3] proposed a system that is able to detect human falls automatically and these falls can be segmented from other different activities. CSI has also been used in breathing detection [15] with the understanding of the Fresnel Zone between transmitter and receiver.

One of the major challenge for a CSI system is the changes in the surrounding environment which can significantly affect the communication channel. Several approaches have been used to eliminate the training phase in each new environment. For example, [19] computes different metrics from the CSI measurements such as mean, standard deviation, etc., for people counting applications which requires only requires training within that specific environment. [4] uses the RSS information for gesture recognition by extracting the frequency component with wavelet transform, and no calibration is required. Similarly, [14] converts the CSI into Doppler spectrograms using STFT, thus avoiding any calibration. A common approach in

TABLE I: Overview of some Recent WiFi Sensing Works

Reference	System	Signal Processing	Machine Learning	Application	Performance
[6]	Distributed WiFi AP	FP, compressive sensing, cluster	N/A	indoor localization	90% error of 2.7 mover 26 APs
[12]	CSI	Wavelet-based denoising, multipath mitigation	PCI, subcarrier selection, DTW	finger gesture recognition	93% accuracy over 8 finger gestures
[14]	CSI	PCA, thresholding	DWT, HMM	activity recognition	96.5% accuracy over 9 activities
[2]	CSI	STFT, spectrogram superimposition	SVM (Radial Basis Function (RBF) kernel)	activity recognition	average false acceptance rate and false rejection rate of 8.05% and 9.54%
[3]	CSI	interpolation, segmentation	8 empirical features, SVM	fall detection	91% of sensitivity and 92% of specificity
[15]	CSI	chest motion modeled as Fresnel zone	N/A	breathing detection	show ability in 1 m from different orientations
[16]	PWR	CAF, CLEAN	N/A	long distance detection	detect a moving person at 17 m away and TTW
[17]	PWR	ECA, CAF	N/A	outdoor detection	detect a running person and a moving car
[18]	PWR	CAF, CLEAN	N/A	finger gesture and activity recognition	feasibility demonstration
[9]	PWR	CAF, CLEAN, micro Doppler extraction	N/A	breathing detection	detection range up to 1 m at different orientations
[10]	PWR	CAF, CLEAN	HMM, K-means clustering	activity recognition	80% accuracy with unsupervised learning over 6 activities

the studies mentioned above is that they convert the RSS/CSI into the form of Doppler information to avoid calibration in the dynamic environment.

B. Passive WiFi Radar

Aside from the CSI systems, passive radar has been extended to exploit WiFi access points as illuminators of opportunity. Passive radar has a long history in airborne tracking and detection, but only over the last decade has it been used for personnel detection [16]. The underlying concept of passive radar is to exploit the signals from third-party transmitters, to measure the time difference between the signal arriving directly to a reference receiver and the signal arriving via reflection from the object through a synchronised surveillnace channel.

Signal processing for passive WiFi radar is more straightforward than CSI. It uses a Cross Ambiguity Function (CAF) to generate range (relative distance) and Doppler (relative velocity) information. However, due to the limited bandwidth of WiFi systems (20-40 MHz), the Doppler information is mainly used for indoor scenarios. The advantage of Doppler information, as discussed above, is that no calibration for the surrounding environment is required. An early attempt of the passive WiFi radar in [16] shows the feasibility of using WiFi signal to detect personnel at a stand-off distance under Through-The-Wall (TTW) condition. [17] investigates the passive WiFi radar for an outdoor scenario, and successfully detects both range and Doppler information for a moving car and a running human. [18] built a prototype based on the Software-Defined-Radio (SDR) platform with real-time ability, and showed potential for several applications such as activity and finger gesture recognition. Passive WiFi radar has also been used for breathing detection. For instance, in [9] we demonstrate that micro-Doppler information can be obtained from the chest motion. The performance of activity recognition and breathing detection is affected by the geometry of the transmitter and receivers. Passive WiFi radar for indoor localization is achieved by tracking the Doppler due to a moving object from at least two separated channels [20]. However, the localization accuracy only depends on the Doppler information which will accumulate error over time [20].

The strong direct signal from a WiFi AP is a major source of interference for a PWR system. Both physical (e.g. angular antenna nulling), and post-processing techniques such as adaptive filtering can be used to remove the direct signal interference (DSI). Colone et al [17] propose the Extensive Cancellation Algorithm (ECA) which subtracts the direct signal from the reflected signals based on the least square technique. However ECA has high computational load making real-time processing infeasible. Another work [16] uses a modified 'CLEAN' algorithm to suppress the dominant peak due to the direct signal with a self-ambiguity function which is calculated by the reference channel and this algorithm shares a similar structure to CAF.

III. Overview of WiFi Sensing

A. Signal Model

OFDM symbol is widely used in many WiFi standards such as IEEE 802.11 a/g/n/ac. In an OFDM system, the bandwidth is shared among multiple overlapping but orthogonal subcarriers and due to the small bandwidth, each subcarrier experiences only flat fading in a frequency-selective fading wireless channel. Let the transmitted OFDM signal be defined as:

$$x(t) = \frac{1}{\sqrt{N}} \sum_{n=0}^{N-1} a_n e^{j\frac{2\pi}{T}nt} \tag{1}$$

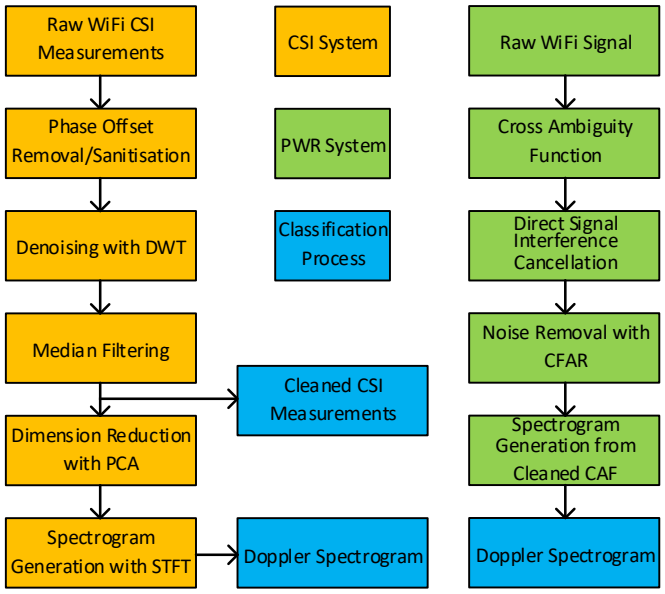

Fig. 1: Block diagram overview of CSI and PWR systems

where T is the OFDM symbol period, N is the number of subcarriers and a_n is the nth symbol in the constellation symbol sequence such as QPSK or QAM. The received signal $y(t)$ consists of both direct signal and multipath reflections. These reflections from a stationary object or a moving person can be represented as a summation of the delayed and phase shifted transmitted signal. The received signal can be written as:

$$y(t) = \sum_{p} A_p e^{j2\pi f_d t} x(t-\tau) + n(t), \tag{2}$$

where p is the number of reflected paths, and A_p, τ, f_d are the attenuation factor, delay, Doppler shift for p-th path respectively, $n(t)$ is the Additive White Gaussian Noise (AWGN).

In the frequency domain, the transmitted signal $X(f_c, t)$ and received signal $Y(f_c, t)$, with carrier frequency f_c are related through the expression $Y(f_c, t) = H(f_c, t) \times X(f_c, t)$, where $H(f_c, t)$ represents the Channel Frequency Response (CFR) at carrier frequency f_c, measured at time t. $H(f_c, t)$ can be expressed as:

$$H(f_c, t) = e^{j2\pi \Delta f_c t} \sum_{p} A_p(f_c, t) e^{j2\pi f_d (t-\tau)}, \tag{3}$$

where $e^{j2\pi f_d(t-\tau)}$ is the phase shift with f_d being the Doppler frequency and τ the propagation delay. $e^{j2\pi \Delta f_c t}$ is the phase difference between transmitter and receiver due to the Sampling Frequency Offset (SFO) and Sampling Time Offset (STO). Although the mechanism of CSI and PWR system is different, however, the key idea of both systems is to detect the changes in the communication channel caused by moving targets and at the same time remove interference from surrounding objects as well as the geometry of transmitter and target reflection.

B. System Model

In this section, we describe of the signal processing for both the PWR and CSI systems for human sensing. This is also summarised by the block diagram in Fig 1. The CSI system is based around communication techniques where information is exchanged between a transmitter and receiver, and PWR system is based on the radar technique which compares the difference between transmitted and reflected signal. For the CSI system, the raw physical layer CSI measurement is obtained from a commercial Network Interference Card (NIC) and stored for off-line processing. Conversely, the raw WiFi signal in the PWR system is measured from a USRP platform, and is down-converted and digitised for real-time processing in a PC.

In order for the receiver to decode the correct transmitted signal in a wireless medium, the propagation characteristics of the channel must be known. In this regard, a training sequence that is known by both the transmitter and receiver is sent in each packet to obtain the channel estimate. This process is often referred to as channel sounding. The channel estimate is known as CSI and for a MIMO-OFDM system, it is a matrix consisting of complex values for each subcarrier. The equalizer uses the CSI to reverse the effects of the channel on the transmitted information such as multipath propagation, attenuation, phase shift, etc. In the IEEE 802.11n standard, the training sequences are known as high throughput long training fields (HT-LTF) and they are sent as part of the preamble for the receiver to obtain the CSI [21]. On the other hand, the PWR system (with the radar technique) correlates the transmitted signal $x(t)$ and received signal $y(t)$ [22] to detect the Doppler shift f_d and propagation delay τ. PWR follows the structure of passive radar system, it has a 'reference channel' to recover the transmitted signal, and several 'surveillance channels' to capture the reflected signal from different angle to provide spatial information.

There are two stages for the classification process in a CSI system. Firstly, the processed CSI measurement, after median filtering, can be directly fed to a neural network. However, this approach is computationally intensive [23], considering the size of the CSI data. Another approach [19], [24] convert the processed CSI data into spectrograms using STFT. Due to the nature of the Doppler information, this approach does not require any calibration process as it is insensitive to static objects. Classification in a PWR system is more straightforward as it directly outputs the Doppler spectrogram which can be used for distinguishing users' activity. This saves a transformation process when compared to the CSI system.

In this work, we focus on the Doppler spectrogram obtained from both systems to train a deep neural network and obtain the classification accuracy for each system. More details on the signal processing of each system are given in sections IV and V.

C. Mechanism

The mechanisms of the CSI and PWR systems in time and frequency domains are illustrated in Fig. 2 and Fig. 3,

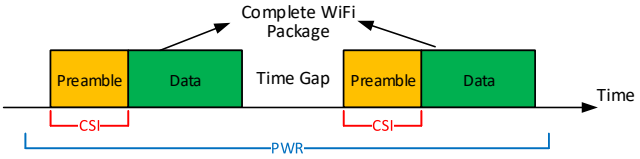

Fig. 2: Demonstration of CSI and PWR mechanisms in time domain.

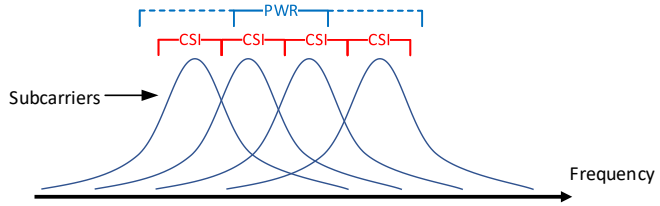

Fig. 3: Demonstration of CSI and PWR mechanisms in frequency domain.

respectively. CSI characterizes how wireless signals propagate from the transmitter to receiver based on the preamble in a WiFi packet. The pre-defined sequence is used to generate the corresponding CSI measurement. The CSI system ignores the data signal and hence does not take full advantage of a whole WiFi packet. In comparison, the PWR system does not require details of the preamble or data in a WiFi packet. To ensure Doppler sensitivity and ensure signal cotent, PWR records signals for a longer duration than CSI. The advantage of PWR system is that it can use both the preamble and data signal, whereas it considers the time gap between two packets to be redundant noise. The activity detection performance of both the CSI and PWR systems depends on the frequency of the received WiFi packets, where the typical default setting of a commercial WiFi AP (10 beacon frames per second) is not sufficient for sensing.

CSI systems make estimates about the communication channel at each subcarrier (in frequency domain). These measurements can provide fine-grained features but they normally have a considerable size. On the other hand, PWR system does not process the OFDM signal on a subcarrier basis but treats each OFDM symbol as one signal. For this reason, the PWR system cannot access the information within each subcarrier. The bandwidth of the PWR system is adjustable from the full WiFi spectrum to a single tone. It is true that the channel information from each subcarrier provides better resolution than the PWR system which processes the Doppler shift from the whole signal instead of individual subcarriers. However, the variations across all subcarriers may not be vastly different.

CSI and PWR have different working principles as shown in Figure 4. The major difference is that the PWR system has an additional channel (reference channel) compared to the CSI system. The function of this reference channel is similar to the preamble signal in the CSI system which aims to recover the original transmitted signal from the WiFi AP. However, the reference channel is unstable in reality since it may not

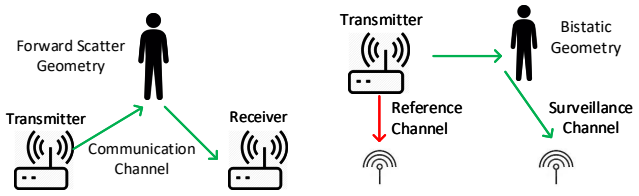

(a) (b)

Fig. 4: Layout: (a) CSI system and (b) PWR system

perfectly recreate the signal due to the moving object reflection and imbalanced RSS level from antenna, although it could be solved by directly tap-off the signal. In comparison, the preamble signal is more reliable than the reference channel to generate the CSI measurement which also simplifies the system to a single channel.

The working principle of the CSI system is that it captures the variation in the communication channel between the transmitter and receiver due to motion. It works best, i.e., it is most sensitive to the variations caused by a human activity when there is a LoS path between the transmitter and receiver. This geometry is also known as the forward scatter, where the angle between transmitter-target and target-receiver is around 180 degrees [25]. However, this geometry is not ideal for a PWR system since the Doppler information is lost at LoS [26], which therefore reduces the system's sensitivity As a passive radar system, PWR performs better in a monostatic geometry, where the the angle between transmitter-target and target-receiver is smaller than 90 degrees [25]. Since the two systems work best in different physical geometries, they have different coverage areas and their Doppler spectrograms will differ for the same geometry.

IV. Signal Processing for CSI System

This section presents the signal processing techniques used in the CSI system including phase calibration for SFO and STO, noise removal, signal compression and signal transform.

A. SFO and STO Removal (Phase Calibration)

In practical WiFi systems, the raw CSI measurements are affected by phase offsets as the hardware and software are not ideal. STO and SFO are caused by non-synchronized sampling clocks and frequencies between the transmitter and receiver, respectively. Phase shifts in the spatial domain and frequency domain provide useful information such as ToF and AoA which can be used for localization and tracking purposes [5]. Since in this work we focus on human activity sensing, the time-domain CSI amplitude variations are enough for this purpose as they exhibit different patterns for different activities. Nonetheless, the phase is calibrated as in [27] where a linear transformation is applied to the raw phase data to eliminate the phase offset. The measured phase $\hat{\phi}_i$ of the ith subcarrier be expressed as:

$$\hat{\phi}_i = \phi_i - 2\pi \frac{k_i}{N} \delta t + \beta + Z, \tag{4}$$

where ϕ is the true phase, β is the phase offset due to carrier frequency offset, δt is the timing offset between the transmitter and receiver, k_i is the index of the ith subcarrier and Z is the measured noise. In the Intel 5300 CSI tool [28], $i \in \{1, 30\}$ and N is the FFT size. For example, $N = 64$ for a 20 MHz WiFi channel in IEEE 802.11 a/g/n. The terms δt, β and Z make it difficult to obtain the true phase from WiFi NICs. The phase obtained from the raw CSI measurements is corrected by first unwinding it and then applying a linear transformation. The main idea is to remove the terms δt and β by considering the phase across the whole frequency band [27].

B. Noise Reduction

Since raw CSI data is noisy in nature, we adopt the Discrete Wavelet Transform (DWT) technique to filter out in-band noise and preserve the high frequency components, thereby introducing less distortion to the signal. DWT-based noise filtering consists of transforming the signal into the wavelet domain whereby the signal is divided into several frequency levels called wavelets that consist of the detail and approximation coefficients [29]. These can be mathematically represented as [5]:

$$y_{1,\text{low}}[n] = \downarrow Q \left[\sum_{k=-\infty}^{\infty} x[k] g[n-k] \right], \tag{5}$$

$$y_{1,\text{high}}[n] = \downarrow Q \left[\sum_{k=-\infty}^{\infty} x[k] h[n-k] \right], \tag{6}$$

where $y_{1,\text{low}}[n]$ and $y_{1,\text{high}}[n]$ are the approximation and detail coefficients, respectively, k denotes the frequency index, $x[k]$ is the input signal, $\downarrow Q[\cdot]$ represents a downsampling filter, $g[n]$ is a low-pass filter and $h[n]$ is a high-pass filter. The highest wavelet level is considered as noise. For each level, the noise and threshold for that level are estimated. The threshold is adapted for lower wavelets and the noise is removed in all levels without introducing significant distortion to the signal. In addition to DWT denoising, 1-D median filtering is also applied to the signal to remove any unwanted transients or spikes in the signal, especially when no activities were performed and the signal should be stable in this case.

C. Data Reduction

The raw CSI measurements were collected on a device equipped with the Intel 5300 NIC with three receiving antennas. For each pair of transmitting antenna and receiving antenna, we obtain CSI values from 30 OFDM subcarriers using the Linux CSI tool [28]. Therefore, if we have one transmit and three receive antennas, we obtain $1 \times 3 \times 30 = 90$ complex CSI values for each packet. The packet sampling rate was set at 1 kHz and hence in one second, we obtain 1000 packets each of size 90. This results in a large amount of data that needs to be processed and fed to a learning algorithm for classification. Therefore, dimension reduction is necessary in a CSI system. In this work, the widely used PCA dimensionality reduction and denoising technique has been adopted. PCA is used to identify the time-varying correlations between CSI streams which are then optimally combined to extract components that represent the variation caused by human activities.

The number of PCs, R, is empirically selected to achieve a good trade-off between classification performance and computational complexity [11]. Following DWT denoising, the first two or three PCs are sufficient to capture most of the variance in the CSI data stream [29]. Similar to [11], in the CSI system we extract the first six PCs. However, the first one is safely discarded since it contains a lot of noise and will not result in any loss of information [2], [11], [30]. Therefore, only the next five PCs are retained for further processing.

D. Doppler Spectrogram Generation

CSI measurement is highly sensitive to the surrounding environment and radio-frequency reflections from the human body exhibit different frequencies when performing different activities. These frequencies can be distinguished in the time-frequency domain (spectrogram) by applying STFT to the PCA-denoised signal. Basically, the STFT applies a sliding window to obtain equally-sized segments of the signal and then performs FFT on the samples in each segment. The STFT of a time-domain input signal, $x[n]$, is given as:

$$X(t,k) = \sum_{n=-\infty}^{\infty} x[n] w[n-t] e^{-jkn}, \tag{7}$$

where t and k denote time and frequency indices, respectively, and $w[n]$ represents a window function (e.g., Hamming window). The spectrogram has three dimensions, namely, time, frequency, and FFT amplitude. The Doppler spectrogram from STFT identifies the change of frequencies over time. The window size for FFT determines the trade-offs between frequency and time resolution. For instance, a larger window size results in a higher frequency resolution but lower time resolution. The spectrograms are generated from the five PCs which are then averaged to obtain the final spectrogram. Unlike Doppler radar, the CSI spectrogram does not associate negative frequencies and hence the direction information is not available.

V. Signal Processing for PWR System

PWR is a special-case of biststic radar [26] which has its origins in airborne surveillance. This section outlines the details in the signal processing for the PWR system including the cross-ambiguity function (CAF), CLEAN algorithm and CFAR for noise reduction.

A. Cross Ambiguity Function

The PWR system consists of two synchronised receiver channels; a surveillance channel $S_{sur}(t)$ which measures targets signals from the monitoring area, and a reference channel $S_{ref}(t)$ which records the signal from the WiFi access point. CAF is processing is employed to obtain the range τ and Doppler f_d information by taking the Fast Fourier Transform (FFT) of the cross-correlated signals from surveillance and reference channels. Due to the limited bandwidth in WiFi,

the range resolution is not sufficient for indoor applications. Doppler resolution is defined by the integration of time T_i as: $\Delta f_d = 1/T_i$. This allows the Doppler resolution to be adjusted for detecting human activities. The CAF equation can be written as:

$$CAF(\tau, f_d) = \int_0^{T_i} x(t) y*(t-\tau) e^{j2\pi f_d t} dt \quad (8)$$

where $*$ denotes a complex conjugate operation. Equation (8) requires a high computational load due to the long FFT which is not suitable for real-time processing in our system. Thus, the batch processing [18] has been used for complexity reduction. This is achieved by dividing a long sequence into several short batches so that the cross-correlation and FFT processes are faster. The CAF with batch processing can be expressed as:

$$CAF(\tau, f_d) = \sum_{n=0}^{N_b-1} \int_0^{T_b} x_n(t) y_n^*(t-\tau) e^{j2\pi f_d t} dt \quad (9)$$

where N_b is the number of batches, T_b is the batch length and n is the index of the beacon. In order to obtain better performance, the reference channel was poiniting towards the WiFi AP in our experiments to make it free from interference due to human activities.

B. Direct Signal Cancellation

Note that the PWR system does not need to remove the SFO/STO as in the CSI system since both the surveillance and reference channels are synchronized through the USRP platform and hence they share the same clock source.

A major drawback associated with PWR arises from the direct signal interference (DSI) component which undergoes perfect correlation with the reference signal, producing large range and Doppler sidelobes that can mask the weaker target echoes. Furthermore, the DSI increases the dynamic range requirement of the system. However, angular nulling with the antenna and interference cancellation techniques in the receiver [5] can be used to suppress the unwanted effects and improve system performance. A modified version of the CLEAN algorithm proposed in [16] is therefore adopted to suppress the DSI in our CAF processing. This CLEAN algorithm shares a similar structure to the CAF process but generates the self-ambiguity surface from the reference channel. This self-ambiguity surface is then used as an estimation of the direct signal.

$$CAF^k(\hat{\tau}, \hat{f}_d) = CAF^k(\tau, f_d) - \alpha^k CAF_{self}(\tau - T_k, f_d) \quad (10)$$

where $CAF^k(\hat{\tau}, \hat{f}_d)$ is the cleaned surface at the k iteration, CAF_{self} is the self ambiguity surface, α^k and T_k are the amplitude and phase shift of maximum peak in the kth CAF surface. The CLEAN algorithm is implemented in the same way as the CAF process due to their similar structure.

C. Noise Reduction

After the CLEAN algorithm, we can still observe some noise in the CAF surface. One of the main reasons is that the CAF process over the time gap shown in Fig. 2 may introduce some noise. Furthermore, the CAF may be incorrectly processed due to strong interfering WiFi signals from other APs or weak received signal from the desired AP. One common solution is to apply CFAR to estimate the background noise distributions as follows:

$$\Lambda = \frac{1}{N_\tau \cdot N_{f_d}} \sum_{i=1}^{R_\tau} \sum_{j=1}^{R_{f_d}} CAF(\tau_i, f_{dj}) \quad (11)$$

where Λ is the threshold mapping for CAF. i and j are the indices for range and Doppler bin, respectively, N_τ and N_{f_d} are the training length in range and Doppler bin, respectively. This threshold mapping is then used for normalizing the power and remove the noise as $P(i,j) = |CAF(i,j)|^2/\Lambda$. $P(i,j) < 1$ implies no motion and the corresponding point in CAF is replaced with zeros. Otherwise, it is inferred that an activity has occurred.

TABLE II: System Implementation

System	CSI	PWR
WiFi Signal	2.4 GHz (channel 1)	2.4 GHz (channel 6)
Hardware	Intel 5300 WiFi [28]	NI USRP-2921 [31]
Subcarrier/bandwidth	30 (out of 56) subcarriers	1 MHz (out of 20 MHz)
Antenna	Omni-directional (6 dBi)	Directional (13 dBi)
Packet Rate	1000 per second	1000 per second
Measurement Rate	1000 Hz (same as packet rate)	10 Hz
Real-time Processing	No	Yes
Output Data Size per Second	90k: 1(tx) $\times$ 3(rx) $\times$ 30(sub carriers) $\times$ 1000(packets)	30k: 100(Doppler bin)$\times$30(range bin) $\times$ 10(sliding window)

VI. System Implementation & Experiment

A. System Implementation

To enable a fair comparison between the CSI and PWR systems, we implemented both systems with almost the same settings in terms of hardware as well as the firmware configurations in the WiFi AP. Details of both systems are provided in Table II. The widely used network card, Intel 5300 [28], has been used in our CSI system. The PWR system was built based on our previous work [10]. The front-end RF hardware includes two NI USRP-2921 [31] for wireless signal acquisition and the measured data is transferred to a computing unit (a laptop in this work) through a Gigabyte Ethernet port. Recall that the Intel 5300 Linux CSI tool extracts the CSI measurements from 30 out of 56 subcarriers for each transmit-receive antenna pair, which were stored on a computing unit for off-line processing. The CAF process in the PWR system does not require the entire WiFi spectrum. A bandwidth of 1 MHz was found to be a trade-off between the PWR's system performance and stability. Signal processing for the PWR system was implemented within LabVIEW, with a low-complexity design for CAF processing and CLEAN algorithm. The two systems were synchronized to an external NTP time server to provide timestamped measurements.

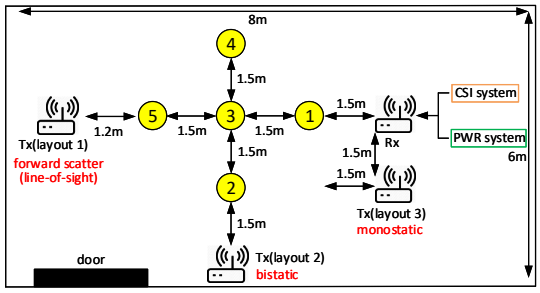

Fig. 5: Experiment layout

Both systems were running in the 2.4 GHz but on different channels to avoid interference. This is because the CSI system continuously pinged the transmitter (AP) to obtain the CSI packets. This two-way communication interferes with the PWR system unless they operate on different channels. The packet rate was set at 1000 per second for both systems to ensure the best activity detection performance can be achieved in both systems. Measurement rate represents the number of system output per second. The measurement rate for the CSI system is based on the number of received packets per second, which is 1000 Hz. However, for the PWR system, it is limited by the amount of baseband signal that can be processed by the computing unit. The measurement rate of the PWR system was set at 10 Hz.

B. Experiment Layout

All measurements were carried out within an office area and the experiment layouts are illustrated in Fig 5. The monitoring area was approximately 8m x 6m with computers and office furniture in the surroundings. To compare the detection performance of the two systems with different geometries, the location of receive antenna remained the same throughout, whereas the WiFi transmitter was moved in each layout as per Fig. 5. Layout 1 refers to the scenario whereby the transmitter-object-receiver alignment is around 180 degrees. This forms a forward scatter geometry which is also known as the line-of-sight. Layout 2 is when the transmitter-object-receiver is around 90 degrees and this forms a bistatic geometry. Layout 3 is when the transmitter-object-receiver is less than 45 degrees and this is known as a monostatic geometry. Five testing positions were used during the experiments and they were separated by 1.5 m from each other. These points are used to evaluate the effect of the system geometry on the activity classification accuracy.

C. Dataset

In this pilot study, we conducted six basic activities, namely, walking, standing from a chair, sitting on a chair, laying down on the ground, standing from the ground and picking up a small object from the ground. The descriptions of the above activities are given in Table III. We applied a sliding window to the Doppler spectrograms and extract 4 seconds of Doppler data for each measurement, no matter the difference

TABLE III: Activity Description

	Activity	Description
(1)	walking	walking in the direction of 1-2-3, 2-3-4; this represents a long, high-level body movement
(2)	sitting	sitting to a chair at position, 1,2,3,4,5; this represents a short, medium-level body movement
(3)	standing	standing from a chair at position, 1,2,3,4,5; this represents a short medium-level body movement
(4)	laying	laying down to floor at position, 1,2,3,4,5; this represents a long low-level body movement
(5)	standing from floor	standing from floor at position, 1,2,3,4,5; this represents a long, low-level body movement
(6)	picking	picking up small items at position, 1,2,3,4,5; this represents a short, medium-level body movement

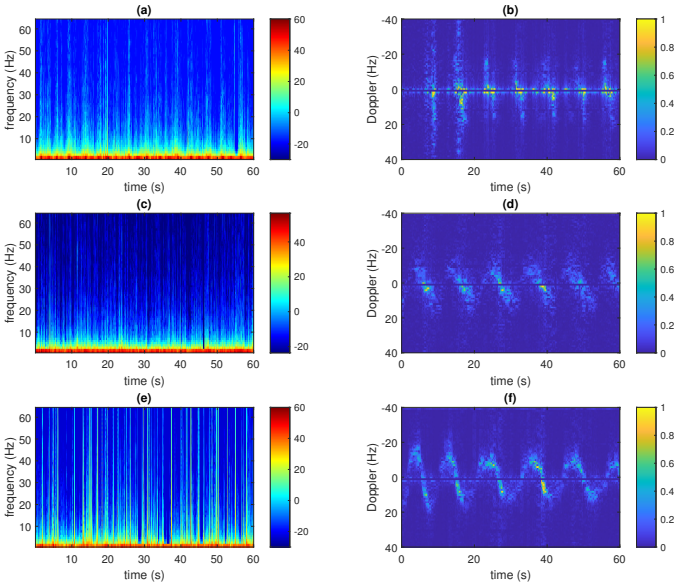

Fig. 6: Walking spectrogram obtained from (a) CSI system in layout 1, (b) PWR system in layout 1, (c) CSI system in layout 2, (d) PWR system in layout 2, (e) CSI system in layout 3 and (f) PWR system in layout 3

in the activity duration. Five volunteers (four males and one female) of different age groups (ranging from 22 to 30) were involved in the experiments. Each activity was performed in a random fashion with no particular orientation with respect to the receiving antenna. This allows greater diversity in the data collection, which is also representative of real-world day-to-day activities. In this work, we have collected a total of 1,122 data samples from the six activities. Among these, layout 1 has 138 samples, layout 2 has 826 samples and layout 3 has 158 samples.

VII. Experimental Results

In this section, the activity recognition performance of both the CSI and PWR systems is presented. A simple 2D Convolutional Neural Network (CNN) has been used as the classifier. The CNN includes one convolutional layer, one max-pooling layer and two fully connected layers. Since the input

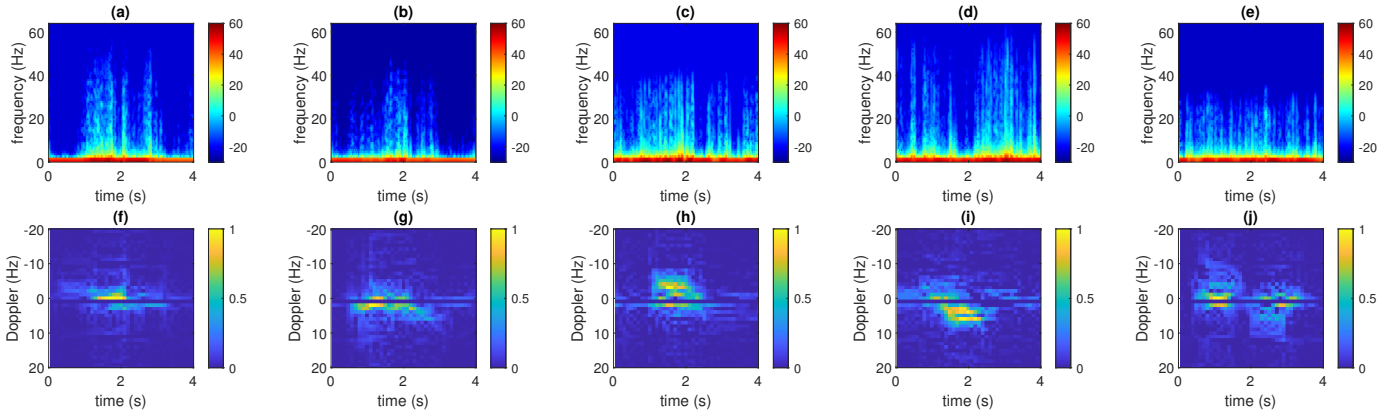

Fig. 7: Spectrogram obtained from layout 2 by CSI system: (a) sitting, (b) standing, (c) laying, (d) standing from floor, (e) picking and from PWR system: (f) sitting, (g) standing, (h) laying, (i) standing from floor, (j) picking

data size is different for the two systems, some parameters are different in the classifier.

A. *Spectrogram Comparison*

Firstly Fig 6 presents the difference in the walking spectrograms obtained from the CSI and PWR systems for all three layouts. Test subjects walked along positions 2-5-8 repeatedly at a constant speed. As can be seen from Fig 6, the subsequent spectrograms have similar signatures in the CSI system with a dominant high Doppler frequency which we attribute to movement of the torso, and small frequencies which are related to the movement of the limbs.

In comparison, Doppler signatures for walking in the PWR system present a significantly different footprint in terms of Doppler profile, shift and amplitude. The can be explained as the PWR system is highly sensitive to the geometry of the transmitter and receiver locations. The PWR spectrogram in layout 1 (Fig 6(b)) shows very low Doppler shift since the relative velocity between the transmitter-object and object-receiver is almost zero when the PWR system operates in line-of-sight. The spectrogram in layout 2 (Fig 6(d)) and layout 3 (Fig 6(f)) have clearer Doppler signatures and more significant Doppler shifts.

In addition, the spectrogram from the CSI system does not contain information regarding the walking direction, whereas the sinusoidal wave in PWR system clearly indicate its velocity and direction. This is because the CSI measurement represents a short period of time (the duration of preamble signal) of channel which gives the information about instant frequency changes, thus no direction information. The PWR system has an integration time of 1 second which is sufficient to observe the direction of the object. However, the PWR system is less sensitive to micro Doppler when capturing a large movement, for example, the limbs' Doppler during walking. This is because the dominant Doppler pulse can easily mask the micro Doppler pulses.

Fig 7 presents spectrograms for the other five activities examined by the two systems. As it can be seen, the frequency

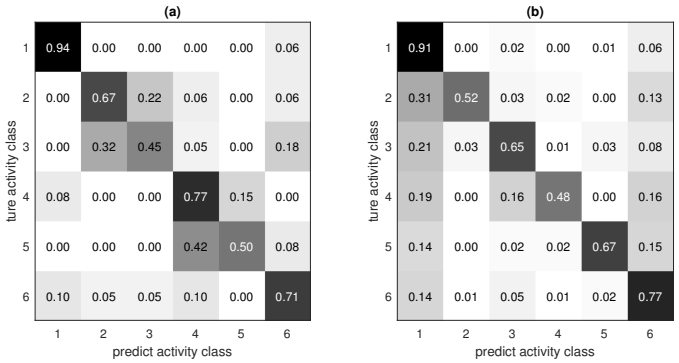

Fig. 8: Classification matrices for activity recognition for combined layouts 1,2,3 in (a) CSI system and (b) PWR system

shifts in the CSI's spectrograms are lower than that in the walking spectrogram as in Fig 6. Generally, all frequency shifts or Doppler shifts in Fig 7 are lower than that in Fig 6 due to the relatively slower body motion. There are some lower frequency shifts in the CSI spectrogram which relate to part body movement. For example, the short and weak frequency shifts when standing from chair (Fig 7(a)), which has similar shape to standing from floor (Fig 7(c)). While, the picking up activity (Fig 7(e)) has the lowest frequency shift.

There are more patterns can be found in PWR's spectrograms from certain activities. For example, sitting to a chair (Fig 7(f)) and laying down to the floor (Fig 7(h)) both has a negative Doppler shape, due to both activity contains a downward body movement. This can be also observed from the standing from chair (Fig 7(g)) and standing from floor (Fig 7(i)), where both contains a positive Doppler shape. Picking up activity contains two part movements, bending over and straightening up the body. As expected, we can see a negative shape following with a positive shape (Fig 7(j)).

B. Classification Accuracy Versus Activity

We first conduct the classification results for all activities in terms of different positions or layouts. 80% of the dataset was chosen randomly and used for training, and the remaining 20% was used for testing. The overall accuracy for the CSI system is 67.3% and the PWR system has almost similar accuracy at 66.7%. These accuracies are lower than those achieved in studies like [**?**], [2], [10], [32] (more than 90% in accuracy). The reason for the low accuracy is because of the mixture of forward scatter (LoS), bistatic and monostatic (NLoS) layouts that result in different Doppler signatures as presented in Fig 6. Also, the change of measurement position means the variation in reflection power at the receiver side would cause the strength of the Doppler signal to become unstable. Nevertheless, this accuracy is still acceptable, it is considered a benchmark when different physical layouts and positions are mixed up together.

The confusion matrices for the CSI system and PWR system are shown in Fig 8(a) and Fig.8(b), respectively. As it can be seen, both systems has the best classification result from activity 1 (walking) that is more than 90%. This is because the walking activity contains higher Doppler shifts than other activities in any directions or layouts. The second best result is observed from activity 6 (picking) which is more than 70%. Other four activities have relatively low accuracy. CSI system has the worst performance from activity 3 (standing) and activity 5 (standing from floor), whereas the PWR system has the worst performance from activity 2 (sitting) and activity 4 (laying down). Moreover, the wrong predictions in the CSI system mostly happen between the pair of activities like sitting on a chair and standing from a chair, laying down and standing from floor. The reason is because the CSI system measures Doppler shift in a short time and is therefore more sensitive to activities with different time duration. In comparison, most incorrect predictions in the PWR system occur for the walking activity. This is because the PWR system has longer integration time (1s in this work), so that long duration activities are easier to distinguish. This accuracy could be easily improved by choosing the appropriate layout for each system.

One of the major limitations is the geometry of transmission and reception. Thus, it is interesting to evaluate the activity recognition accuracy in different physical setups. To evaluate such performance, both the training and testing data were used within the same layout. The results are shown in Fig 9. As expected, the CSI system has the best performance in layout 1 at 91% and worst performance in layout 3 at 62%, whereas the PWR system has the best performance in layout 3 with an accuracy of 91.1% and worst in layout 1 with an accuracy of 60%. Both systems have almost similar accuracy in layout 2 around 70%, which is more than the accuracy in Fig 8. As mentioned previously, the CSI and PWR systems have different mechanisms in processing the WiFi signal. The CSI system has better performance in the forward scatter (LoS) layout while the PWR system has better performance in the monostatic layout. These results demonstrate the coverage of

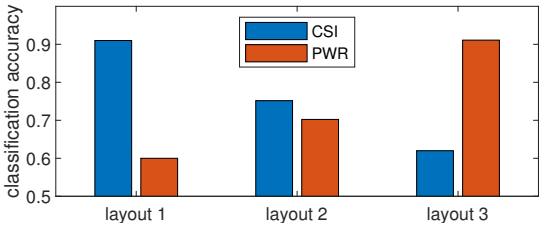

Fig. 9: Classification versus three layouts

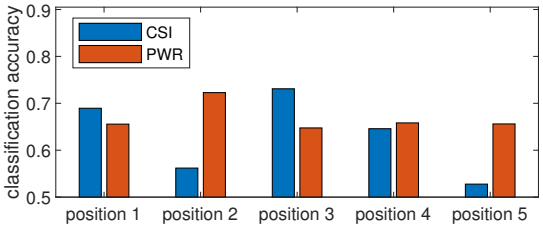

Fig. 10: Classification versus different positions

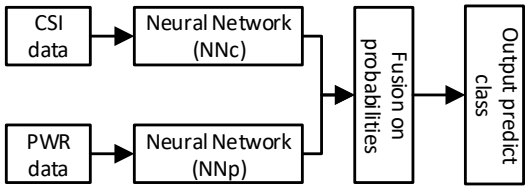

Fig. 11: Fusion framework for two systems

the two systems that can be used in real applications.

Afterwards, we calculate the accuracy over each position as demonstrated in Fig 5. In this experiment, we tested the data for a specific position and trained the data for all other positions (excluding the walking activity which covers several positions). The classification accuracy for each position is shown in Fig 10. As it can be seen, there are some variation in accuracy in each system. More specifically, the CSI system has the worst performance at positions 2 and 5, where both are below 60%. The CSI system works best at position 3 which is close to a LoS layout. In comparison, the PWR system has a more balanced performance across all positions since the bistatic angle is relative similar. The spectrograms in positions 2 and 5 have relatively similar Doppler signatures. These results show that CSI and PWR systems have slightly different coverage, and therefore a fusion of the two systems could improve the performance in weaker positions.

C. Combined Classification accuracy

So far, classification results are calculated separately for the two systems. As discussed before, there are considerable differences in classification accuracy in terms of system layout and position. Here, we combine the results from both systems to further improve the accuracy for WiFi sensing. Inspired by the work in [33], a simple fusion framework has been used as shown in Fig 11. Here we export the probabilities, P_c and P_p, for each activity from the Neural Networks used for the CSI

TABLE IV: Combined Accuracy

Dataset	Method	CSI	PWR	Combined
layout 2	Addition	75.7%	72.8%	79.8%
layout 2	Multiplication	75.7%	72.8%	74.0%
layout 1,2,3	Addition	67.3%	66.7%	74.2%
layout 1,2,3	Multiplication	67.3%	66.7%	70.2%

and PWR systems, respectively. We set the two systems with same weight, and use two methods to calculate the combined probabilities, P_f; the addition method where $P_f = \frac{1}{2}(P_c + P_p)$ and the multiplication method where $P_f = P_c * P_p$.

The combined accuracy for layout 2 and layouts 1,2,3 are given in Table IV. We followed the same procedures as discussed in Section VII-B. As it can be seen, there are some improvements in the combined accuracy as compared to the accuracy obtained from the CSI and PWR systems separately. In layout 2, the combined accuracy using the addition method is 79.8% which is 4.1% and 6.0% higher than the accuracy of each individual system, whereas the multiplication method results in a slightly lower combined accuracy. The combined accuracy shows even better improvement in layout 1,2,3 which achieves 74.2%. In addition, these improvements are generated using a simple fusion framework based on the probabilities from the two systems. It is envisioned that a more robust fusion process using the CSI and PWR data could further improve the classification accuracy.

For layout 1 and layout 3, the imbalanced performance between the two systems makes the fusion process ineffective. In some cases, the fusion process could lower the original accuracy since we consider equal weights in this work.

VIII. Discussion

This section presents the challenges that we faced during the implementation and experimentation with both systems. Future improvements to the in hardware setup for an integrated measurement system, signal processing and machine learning algorithms are also discussed.

A. Resilience to Environmental Changes

WiFi signals are very sensitive to various factors such as the geometry of transmission and reception, environmental conditions and operational parameters of the communication network It is crucial to build a robust WiFi sensing system that can be adapted for different environments and WiFi AP settings (e.g. bandwidth, transmit power, MIMO capability, etc) but this represents a challenge. For example, the direction and orientation of the person with respect to the WiFi AP and receiver can change continuously. The distance between the person and WiFi AP could also be varied. In practical scenarios, there may be multiple people or other moving objects around that could block the reference channel as well as the baseline (LoS) between the transmitter and receiver. It is very challenging for WiFi sensing systems to have the generalization ability to automatically adapt to new and unseen data. In other words, a WiFi sensing system should also work when the device is placed in a new environment, unknown location and operate for new talents.

For a CSI system, it requires a process to understand the surrounding environment during a static measurement. However, this process may have high complexity and hard to operate in a real-world application. One solution is to convert the CSI measurement into Doppler spectrograms to calculate the change in frequency. However, this does not entirely solve the problem as CSI's spectrogram does not show the direction of motion. In comparison, the PWR system directly outputs a Doppler spectrogram which is less sensitive to the static objects and we can use a previously trained model for a new environment. However, the PWR system needs to overcome the challenge where two channels are required. The re-creation of the transmitted signal should be improved through a robust algorithm instead of using a physical channel.

B. Efficiency in Spectrum Usage

The fundamental purpose of WiFi is for wireless communications. Sensing is a peripheral application which can either be used to optimise the performance and quality of service of the network, or secondary applications in healtcare, IoT, security etc. The majority of previous studies which have examined CSI based sensing systems [7], [11], [12], [24] use a high packet rate to achieve good performance. However, the high packet rates can be regarded as the exchange of redundant information which occupy a considerable amount of the already-limited WiFi spectrum. This in turn affects the network performance, degrading the quality of service for connected users. Moreover, sending unnecessary packets for CSI measurements influences not only the measuring device but also the nearby WiFi devices, since the packets occupy WiFi resources in both time and frequency domains. In contrast, the passive nature of the PWR system means that no extra packets are transmitted for sensing purposes. This minimizes the influence to communication systems, but the PWR's performance is highly dependent on the density of the WiFi packages which might be a problem when the data traffic through the AP is low.

In addition, the CSI system does not take full advantage of a WiFi packet. Recall from Fig 2, the CSI system only uses the preamble signal to obtain the desired CSI but does not have information about the transmitted data signal. Despite that the PWR system can capture the whole packets, however, it also captures the time gap between packets which are redundant for sensing but still has a computational processing overhead. To enhance the detection performance, it is important to maximize the usage of the WiFi package while filtering out the time gap period. This is required for the data signal generation in the PWR system using the reference channel method.

C. Beamforming

The latest IEEE 802.11ac standard use the beamforming technique which could have an adverse impact on both CSI and PWR sensing as it changes the amplitude and phase of the WiFi signals. As a result, the CSI measurements may become

unstable and difficult to process if the beamforming matrix is not available at the receiver side. The PWR system faces more challenges due to the beamforming technique. Traditionally, passive radar works with relatively low bandwidth and uses a single carrier signal like FM radio and analog television. Multiple antennas in the beamforming technique means the aquisition of the PWR's reference channel becomes even more complicated. Acquiring the reference channel using a single directional antenna from a MIMO AP will be challenging since each received signal will have different amplitude and phase. The variation in phase difference may generate erroneous Doppler pulse in the CAF surface and cause similar side-lobe problem in the PWR system. Nonetheless, beamforming can be advantageous for WiFi sensing by providing spatial information in addition to the Doppler and range information. However, current CSI and PWR systems have not used this new technique to generate joint spatial and Doppler data.

D. Challenges in Signal Processing

Using commercial NIC cards, the CSI system can obtain fine-grained CSI measurements directly without any further processing. However, the size of the CSI measurements (shown in Table II) is proportional to the number of antennas and packet rate. This means a huge computational power is required to process such amount of data, although it is possible to reduce the size of the data using techniques such as PCA, which captures most of the variance among the subcarriers over multiple antennas in only a few principal components. On the other hand, the raw CSI measurement is too noisy to be used directly for sensing purposes and hence the CSI signal processing represents a very important engineering task. The processing of CSI measurements to obtain meaningful information such as Doppler, range, AoA, ToF, etc, is necessary and it is worthwhile to develop algorithms which are useful for joint activity recognition and localisation applications.

From the Doppler spectrograms, we realize that the traditional CAF process (Equation 8) in the PWR system could not deliver sufficient range resolution for human sensing due to the limited WiFi bandwidth. Also the integration time (one second in this work) which defines the Doppler resolution, is too long for activities consisting of hand gestures. It is believed that a more efficient CAF processing with time synchronization (to extract effective WiFi signal) could further improve the PWR system in both range and Doppler resolutions. Moreover, the CSI system has a low sensitivity to activities performed far from the baseline while the PWR system has a low sensitivity to activities performed close to the baseline. Thus, information fusion from both systems could significantly improve the coverage for WiFi sensing.

E. Challenges in Machine Learning Algorithms

Machine learning algorithms in WiFi sensing face several challenges. Firstly, the training data available for some activities such as falling down (especially by elderly people) are difficult collect and may be insufficient to train a model due to under-fitting. This is a class imbalance problem [34], where most standard classifier learning algorithms assume a relatively balanced class distribution. Such a situation represents a challenge in current WiFi sensing works [10], [11], [14] and thus a different approach [34] is required for the imbalanced activity classes.

Secondly, a large dataset is required to properly train a classifier, taking into account various factors like transmit/receive geometry, abnormal activities and different height/weight of people which could potentially change the Doppler pattern for a given activity. This may not be feasible since the data collection process will be time consuming and may incur a high cost. However, two common solutions are available, namely, model-based algorithms such as Finite Difference Time Domain (FDTD) [35] which studies the physical theories or statistical model of the target, and learning-based algorithms such as Generative Adversarial Network (GAN) [36] which generates new datasets based on a pre-trained network. Some early works like [36], [37] have shown the potential of using generated Doppler spectrum to improve the accuracy in activity recognition. However, current works applying these algorithms are still in the early stage and they focus on simple activities performed mostly in a static environment (very controlled experiments).

Another challenge is the cross-device/sensor in WiFi sensing. Multiple WiFi devices can be combined together to achieve a higher performance and efficiency. Due to the rapidly increasing demand in wireless data, there will be more WiFi devices available in different scenarios. These devices are location separated which could provide extra information for cross-device sensing. In addition to WiFi devices, many other types of sensors such as cameras, mobile phones, laptops, IoT devices, etc., can be used for cross-sensor sensing. The latter can reduce human efforts for training machine learning algorithms. For example, video cameras can be used to generate automatic ground truth labels for the CSI and PWR systems.

IX. Conclusions

In this paper, we present and compare methods based on communications (CSI) and radar (PWR) protocols for activity sensing using WiFi transmissions. We contrast the difference between these systems in terms of fundamental principles and key challenges. We report on a range of human activity data obtained from these two systems in realistic indoor environments and compare the classification accuracy in terms of system and surveillance area geometries The CSI and PWR systems show the best performance in the line-of-sight and monostatic layouts, respectively. Moreover, we have demonstrated that a fusion process on both systems could easily improve the accuracy for activity recognition. Future work includes the development of a more robust system that can combine the advantages of the CSI and PWR systems. Also, the efficiency in spectrum usage and beamforming technique are worth considering in WiFi sensing.

ACKNOWLEDGMENTS

This work was funded under the OPERA Project, the UK Engineering and Physical Sciences Research Council (EPSRC), Grant EP/R018677/1.

REFERENCES

[1] C. J. Caspersen, K. E. Powell, and G. M. Christenson, "Physical activity, exercise, and physical fitness: definitions and distinctions for health-related research." *Public health reports*, vol. 100, no. 2, p. 126, 1985.

[2] W. Wang, A. X. Liu, and M. Shahzad, "Gait recognition using wifi signals," in *Proceedings of the 2016 ACM International Joint Conference on Pervasive and Ubiquitous Computing*, 2016, pp. 363–373.

[3] H. Wang, D. Zhang, Y. Wang, J. Ma, Y. Wang, and S. Li, "Rt-fall: A real-time and contactless fall detection system with commodity wifi devices," *IEEE Transactions on Mobile Computing*, vol. 16, no. 2, pp. 511–526, 2016.

[4] H. Abdelnasser, M. Youssef, and K. A. Harras, "Wigest: A ubiquitous wifi-based gesture recognition system," in *2015 IEEE Conference on Computer Communications (INFOCOM)*. IEEE, 2015, pp. 1472–1480.

[5] Y. Ma, G. Zhou, and S. Wang, "Wifi sensing with channel state information: A survey," *ACM Computing Surveys (CSUR)*, vol. 52, no. 3, p. 46, 2019.

[6] C. Feng, W. S. A. Au, S. Valaee, and Z. Tan, "Received-signal-strength-based indoor positioning using compressive sensing," *IEEE Transactions on mobile computing*, vol. 11, no. 12, pp. 1983–1993, 2011.

[7] C. Yang and H.-R. Shao, "Wifi-based indoor positioning," *IEEE Communications Magazine*, vol. 53, no. 3, pp. 150–157, 2015.

[8] A. Makki, A. Siddig, M. Saad, and C. Bleakley, "Survey of wifi positioning using time-based techniques," *Computer Networks*, vol. 88, pp. 218–233, 2015.

[9] W. Li, B. Tan, and R. J. Piechocki, "Non-contact breathing detection using passive radar," in *2016 IEEE International Conference on Communications (ICC)*. IEEE, 2016, pp. 1–6.

[10] W. Li, B. Tan, Y. Xu, and R. J. Piechocki, "Log-likelihood clustering-enabled passive rf sensing for residential activity recognition," *IEEE Sensors Journal*, vol. 18, no. 13, pp. 5413–5421, 2018.

[11] W. Wang, A. X. Liu, M. Shahzad, K. Ling, and S. Lu, "Understanding and modeling of wifi signal based human activity recognition," in *Proceedings of the 21st annual international conference on mobile computing and networking*. ACM, 2015, pp. 65–76.

[12] S. Tan and J. Yang, "Wifinger: leveraging commodity wifi for fine-grained finger gesture recognition," in *Proceedings of the 17th ACM international symposium on mobile ad hoc networking and computing*. ACM, 2016, pp. 201–210.

[13] W. Xi, J. Zhao, X.-Y. Li, K. Zhao, S. Tang, X. Liu, and Z. Jiang, "Electronic frog eye: Counting crowd using wifi," in *IEEE INFOCOM 2014-IEEE Conference on Computer Communications*. IEEE, 2014, pp. 361–369.

[14] W. Wang, A. X. Liu, M. Shahzad, K. Ling, and S. Lu, "Device-free human activity recognition using commercial wifi devices," *IEEE Journal on Selected Areas in Communications*, vol. 35, no. 5, pp. 1118–1131, 2017.

[15] H. Wang, D. Zhang, J. Ma, Y. Wang, Y. Wang, D. Wu, T. Gu, and B. Xie, "Human respiration detection with commodity wifi devices: do user location and body orientation matter?" in *Proceedings of the 2016 ACM International Joint Conference on Pervasive and Ubiquitous Computing*. ACM, 2016, pp. 25–36.

[16] K. Chetty, G. E. Smith, and K. Woodbridge, "Through-the-wall sensing of personnel using passive bistatic wifi radar at standoff distances," *IEEE Transactions on Geoscience and Remote Sensing*, vol. 50, no. 4, pp. 1218–1226, 2011.

[17] F. Colone, P. Falcone, C. Bongioanni, and P. Lombardo, "Wifi-based passive bistatic radar: Data processing schemes and experimental results," *IEEE Transactions on Aerospace and Electronic Systems*, vol. 48, no. 2, pp. 1061–1079, 2012.

[18] B. Tan, K. Woodbridge, and K. Chetty, "A real-time high resolution passive wifi doppler-radar and its applications," in *2014 International Radar Conference*. IEEE, 2014, pp. 1–6.

[19] S. Di Domenico, G. Pecoraro, E. Cianca, and M. De Sanctis, "Trained-once device-free crowd counting and occupancy estimation using wifi: A doppler spectrum based approach," in *2016 IEEE 12th International Conference on Wireless and Mobile Computing, Networking and Communications (WiMob)*. IEEE, 2016, pp. 1–8.

[20] W. Li, B. Tan, and R. Piechocki, "Opportunistic doppler-only indoor localization via passive radar," in *2018 IEEE 16th Intl Conf on Dependable, Autonomic and Secure Computing, 16th Intl Conf on Pervasive Intelligence and Computing, 4th Intl Conf on Big Data Intelligence and Computing and Cyber Science and Technology Congress (DASC/PiCom/DataCom/CyberSciTech)*. IEEE, 2018, pp. 467–473.

[21] N. Tadayon, M. T. Rahman, S. Han, S. Valaee, and W. Yu, "Decimeter ranging with channel state information," *IEEE Transactions on Wireless Communications*, vol. 18, no. 7, pp. 3453–3468, 2019.

[22] B. Tan, K. Woodbridge, and K. Chetty, "A wireless passive radar system for real-time through-wall movement detection," *IEEE Transactions on Aerospace and Electronic Systems*, vol. 52, no. 5, pp. 2596–2603, 2016.

[23] S. Di Domenico, M. De Sanctis, E. Cianca, F. Giuliano, and G. Bianchi, "Exploring training options for rf sensing using csi," *IEEE Communications Magazine*, vol. 56, no. 5, pp. 116–123, 2018.

[24] K. Qian, C. Wu, Z. Zhou, Y. Zheng, Z. Yang, and Y. Liu, "Inferring motion direction using commodity wi-fi for interactive exergames," in *Proceedings of the 2017 CHI Conference on Human Factors in Computing Systems*. ACM, 2017, pp. 1961–1972.

[25] M. Cherniakov and D. Nezlin, *Bistatic radar: principles and practice*. Wiley Online Library, 2007.

[26] N. J. Willis, *Bistatic radar*. SciTech Publishing, 2005, vol. 2.

[27] X. Dang, X. Tang, Z. Hao, and Y. Liu, "A device-free indoor localization method using csi with wi-fi signals," *Sensors*, vol. 19, no. 14, p. 3233, 2019.

[28] "Linux 802.11n CSI tool," https://dhalperi.github.io/linux-80211n-csitool/, (Accessed on 05/11/2020).

[29] S. Palipana, D. Rojas, P. Agrawal, and D. Pesch, "Falldefi: Ubiquitous fall detection using commodity wi-fi devices," *Proceedings of the ACM on Interactive, Mobile, Wearable and Ubiquitous Technologies*, vol. 1, no. 4, pp. 1–25, 2018.

[30] S. Liu, Y. Zhao, F. Xue, B. Chen, and X. Chen, "Deepcount: Crowd counting with wifi via deep learning," *arXiv preprint arXiv:1903.05316*, 2019.

[31] "Ni usrp 2921," http://sine.ni.com/nips/cds/view/p/lang/en/nid/212995, (Accessed on 05/11/2020).

[32] S. Duan, T. Yu, and J. He, "Widriver: Driver activity recognition system based on wifi csi," *International Journal of Wireless Information Networks*, vol. 25, no. 2, pp. 146–156, 2018.

[33] P. Zappi, T. Stiefmeier, E. Farella, D. Roggen, L. Benini, and G. Troster, "Activity recognition from on-body sensors by classifier fusion: sensor scalability and robustness," in *2007 3rd international conference on intelligent sensors, sensor networks and information*. IEEE, 2007, pp. 281–286.

[34] Y. Sun, A. K. Wong, and M. S. Kamel, "Classification of imbalanced data: A review," *International journal of pattern recognition and artificial intelligence*, vol. 23, no. 04, pp. 687–719, 2009.

[35] J. B. Schneider, "Understanding the finite-difference time-domain method," *School of electrical engineering and computer science Washington State University*, p. 181, 2010.

[36] K.-S. Zheng, J.-Z. Li, G. Wei, and J.-D. Xu, "Analysis of doppler effect of moving conducting surfaces with lorentz-fdtd method," *Journal of Electromagnetic Waves and Applications*, vol. 27, no. 2, pp. 149–159, 2013.

[37] B. Erol, S. Z. Gurbuz, and M. G. Amin, "Gan-based synthetic radar micro-doppler augmentations for improved human activity recognition," in *2019 IEEE Radar Conference (RadarConf)*. IEEE, 2019, pp. 1–5.